

Accurate Measurement of Mean Axon Diameter with Q-space Diffusion MRI

H. H. Ong¹, and F. W. Wehrli¹

¹Laboratory for Structural NMR Imaging, Department of Radiology, University of Pennsylvania School of Medicine, Philadelphia, PA, United States

Introduction

Knowledge of mean axon diameter (MAD) would provide valuable insight into white matter (WM) architecture and pathology. *Q*-space imaging¹ (QSI) offers potential for indirect assessment of white matter (WM) as the Fourier transform of the QSI signal decay contains axon structure information^{2,3}. This information can, instead, be obtained from the echo attenuation. Although WM is too heterogeneous to observe diffraction patterns in *q*-space³, at low *q*-values ($q = (2\pi)^{-1}\gamma G\delta$ (G and δ are the diffusion gradient amplitude and pulse length, respectively), when $q^{-1} \ll \text{MAD}$, the signal decay is given by $E(q) = \exp(-2\pi^2 q^2 Z^2)$ (Eq.1). In this regime, pore size can be estimated by Z (the root mean squared (RMS) displacement of diffusing molecules during a diffusion time Δ)^{4,5}. The use of only low *q*-values obviates the need for high gradient amplitudes, a drawback with QSI⁶. However, $E(q)$ contains signal from extra- and intra-cellular spaces (ECS and ICS). In this work, we use a two-compartment version of Eq.1 to account for ECS and ICS: $E(q) = f_E \exp(-2\pi^2 q^2 Z_E^2) + f_I \exp(-2\pi^2 q^2 Z_I^2)$ (Eq. 2), where f_E and f_I are the relaxation-weighted ECS and ICS volume fractions and Z_E and Z_I are the RMS displacement of diffusing molecules in the ECS and ICS. MAD of WM tracts in mouse spinal cords (SC) was estimated from $E(q)$ at low *q*-values with both Z (Eq.1) and Z_I (Eq.2) for comparison

Methods

Five SC sections (C6-C7) were dissected from perfusion-fixed 8-10 month-old female C57 BL/6 mice. Experiments were performed with a custom-built 50T/m z-gradient and solenoidal RF coil set (4-turn, 3mm i.d.) interfaced to a 9.4T spectrometer/micro-imaging system (Bruker DMX 400 with Micro2.5 gradients and BAFPA40 amplifiers). A diffusion-weighted stimulated-echo sequence was used: 64x64, SW=25kHz, TR=2s, TE/ Δ / δ =17.4/10/0.4ms, FOV/THK=4/1mm, and an ambient temperature of 19 °C. The diffusion gradient was applied perpendicular to the SC long axis in 64 increments of *q* ($q_{\text{max}}=0.82 \mu\text{m}^{-1}$). Normalized *q*-space decay curves were obtained for each pixel and averaged over ROIs (20 pixels after zero-filling image to 256x256) selected within seven WM tracts (Figure 1). After experiments, SC sections from the MRI slice were stained with toluidine blue and optical images were obtained from all WM tracts. The images were segmented into extra- and intra-axonal, and myelin regions with a custom watershed and profile algorithm. MAD was calculated (excluding myelin) assuming a circular area. Histologic WM tract MADs were used to determine the low *q* regime by only fitting $E(q)$ at $q < (\text{MAD}^{-1})/10$ (the first 11 to 5 *q*-values for the smallest to largest WM tract MAD). All fitting was done with a nonlinear minimization algorithm (interior-reflective Newton method) in Matlab. When fitting with Eq.2, the following parameter constraints were applied: $f_E + f_I = 1$ and $Z_E < 8 \mu\text{m}$ (as RMS displacement in ECS cannot be larger than that of free water).

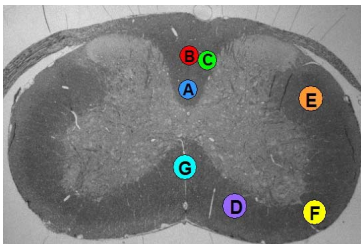


Figure 1. Optical image of SC section showing WM tract locations: A) dorsal corticospinal (dCST), B) gracilis (FG), C) cuneatus (FC), D) rubrospinal (RST), E) spinothalamic (STT), F) reticulospinal (ReSt), G) vestibulospinal (VST).

Results

Figure 2 shows sample fits of data with Eq. 1 and 2. The two-compartment fit has a higher average R^2 suggesting that it may be a better model. Figure 3 shows a plot of experimental MADs estimated from one- and two-compartment fits (Z and Z_I , respectively) vs histologic MAD averaged for each WM tract. An outlier Z_I value for the FC WM tract was removed as it was smaller than the smallest observed MAD. There is excellent linearity and correlation between histology and experiment; Z_I from the two-compartment fit shows closer correspondence with histology. A Bland-Altman plot between the Z_I and histology was generated (not shown) and the 95% confidence interval was from -0.11 to 0.24. No significant correlation was found between Z_E and histologic MAD. The average Z_E was $6.84 \pm 1.19 \mu\text{m}$.

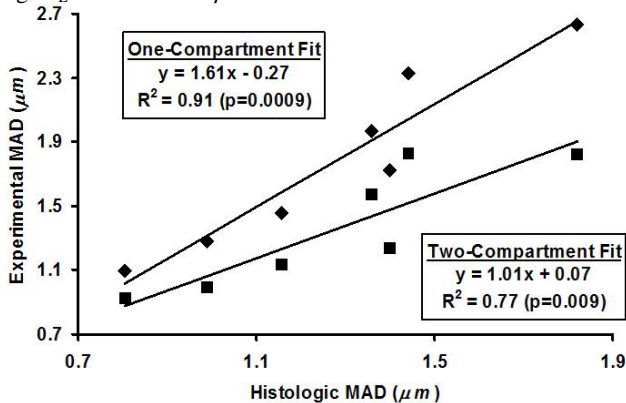


Figure 3. Plot of average WM tract histologic vs experimental MADs (upper curve (diamonds): one-compartment model; lower curve (squares): two-compartment model) with equation of line of best fit.

toluidine blue and optical images were obtained from all WM tracts. The images were segmented into extra- and intra-axonal, and myelin regions with a custom watershed and profile algorithm. MAD was calculated (excluding myelin) assuming a circular area. Histologic WM tract MADs were used to determine the low *q* regime by only fitting $E(q)$ at $q < (\text{MAD}^{-1})/10$ (the first 11 to 5 *q*-values for the smallest to largest WM tract MAD). All fitting was done with a nonlinear minimization algorithm (interior-reflective Newton method) in Matlab. When fitting with Eq.2, the following parameter constraints were applied: $f_E + f_I = 1$ and $Z_E < 8 \mu\text{m}$ (as RMS displacement in ECS cannot be larger than that of free water).

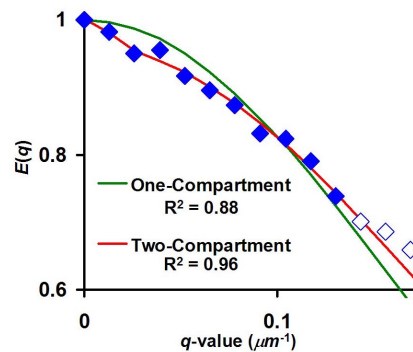


Figure 2. Sample fits of a normalized signal decay curve from dCST WM tract (diamonds). Only the first 11 points were used for fitting (solid diamonds) in order to fulfill the low *q*-value condition.

The protocol was not optimized for fitting $E(q)$ at low *q*-values. Using only 5-11 points for the fits may have introduced errors, especially for the two-compartment fit leading to a lower R^2 in Fig. 3. *Q*-Values greater than $\sim 0.1 \mu\text{m}^{-1}$ would not be necessary as $\text{MAD} \gg 0.8 \mu\text{m}$. That time could be used to sample more points below $q=0.1 \mu\text{m}^{-1}$ or to average the signal in order to improve the fitting. Acquiring images only at low *q*-values is advantageous, because of the relaxed gradient amplitude constraints, as mentioned above, and improved SNR from less diffusion encoding.

Conclusion

This work demonstrates the feasibility of a two-compartment model to extract MAD from low-*q* echo attenuations that yield results in good agreement with histology.

References: 1. Callaghan, PT, *Principles of NMR Microscopy*, Oxford University Press (1991). 2. Assaf Y, et al, *MRM*, **47**:115 (2002). 3. Chin CL, et al, *MRM*, **52**:733 (2004). 4. Price W, *Concepts Magn Res*, **10**:299 (1997). 5. Kimmich R, *NMR: Tomography, Diffusometry, Relaxometry*, Springer-Verlag (1997). 6. Ong H, et al, Proc. ISMRM 15th Scientific Meeting, Berlin, Germany 2007, p. 1533. **Acknowledgements:** NIH grant R21 EB003951